

Observation of wakefield generation in left-handed band of metamaterial-loaded waveguide

S. Antipov,^{1,a)} L. Spentzouris,¹ W. Gai,² M. Conde,² F. Franchini,² R. Konecny,² W. Liu,² J. G. Power,² Z. Yusof,² and C. Jing³

¹Illinois Institute of Technology, Chicago, 60616 Illinois, USA

²Argonne National Laboratory, Argonne, 60439 Illinois, USA

³Euclid Techlabs LLC, Solon, 44139 Ohio, USA

(Received 22 January 2008; accepted 18 April 2008; published online 1 July 2008)

We report on a design of a TM-mode based metamaterial-loaded waveguide. Network analyzer measurements demonstrated a left-handed propagation region for the TM_{11} mode at around 10 GHz. A beamline experiment was performed with the metamaterial-loaded waveguide. In this experiment, a 6 MeV electron beam passes through the waveguide and generates a wakefield via the Cherenkov radiation mechanism. We detected a signal in the left-handed frequency band at 10 GHz. This is an indirect demonstration of reverse Cherenkov radiation as predicted in the work of Veselago [Sov. Phys. Usp. **10**, 509 (1968)] and discussed in the works of Lu *et al.* [Opt. Express **11**, 723 (2003)], Averkov and Yakovenko [Phys. Rev. B **72**, 205110 (2005)], and Tyukhtin *et al.* [IEEE, Proceedings of the PAC, 2007 (unpublished), pp. 4156–4158]. Cherenkov radiation in artificially constructed materials [metamaterials (MTMs)] can provide unusual engineered features that can be advantageous for particle detector design. © 2008 American Institute of Physics. [DOI: 10.1063/1.2948929]

I. INTRODUCTION

The electromagnetic properties of a medium in most cases are characterized by the permittivity ϵ (response to electric field) and permeability μ (response to magnetic field). Typically, ϵ and μ are positive or tensors with positive values for most frequencies of electromagnetic waves. In this case, the phase vector (k) of the wave propagating through the medium forms a right-handed system with the field vectors E and B . The Poynting vector is codirected with k .

Veselago first pointed out that propagation is also possible when ϵ and μ are simultaneously negative.¹ Propagating waves in such double-negative media exhibit several unusual properties. First of all, the phase vector forms a left-handed system with the field vectors. This is why materials with simultaneously negative ϵ and μ are called left handed. In such media, the Poynting vector, which is collinear with the group velocity, is counterdirected to the phase vector. This gives rise to several unusual effects such as the reversed Doppler effect, reversed Cherenkov radiation (CR),^{1–4} and negative refraction.^{1,5}

Materials [metamaterials (MTMs)] with simultaneously negative values for ϵ and μ were artificially constructed in 2000.¹⁰ The arrays of subwavelength elements respond to electromagnetic fields like a medium with dispersive (frequency dependent) permittivity and permeability. Split ring resonators⁶ (SRRs) create an effective magnetic material with μ negative at certain frequencies. Artificial ϵ can be produced, for example, by wire arrays^{7,8} or capacitively loaded strips (CLS).⁹ It is possible to create a MTM with simultaneously negative ϵ and μ .¹⁰

Characteristics analogous to reverse CR were demonstrated^{11,12} by employing current pulses in microwave radiating systems. However, there have been no experiments involving a beam of charged particles. In this paper, we report on the first beam test of a MTM-loaded waveguide. The source used was the 6 MeV electron beam produced by the Argonne Wakefield Accelerator (AWA) photoinjector.¹³

CR is widely used in accelerator physics for beam and particle detector applications. Reverse CR, predicted for double-negative materials, can have unique features useful for beam detection.^{2–4,19} MTMs can be used as an engineered medium for detectors designed to produce radiation that counterpropagates with respect to the particle beam source within a selected frequency band. Originally, MTMs were produced for microwave frequencies using printed circuit board (PCB) techniques. During the past seven years, MTMs were realized in the terahertz range and up to optical frequencies [see, for example, Ref. 14 and review Ref. 15]. Optical MTM would be perfect for Cherenkov detectors, which operate generally in the optical region. To understand the physics of the process, we worked with microwave MTMs because they are easier to manufacture.

We have designed and manufactured a double-negative MTM similar to those developed by other groups [e.g., Ref. 9]. In Refs. 16 and 17, we reported our first MTM design and in Ref. 18 we reviewed our plans for accelerator-related MTM research. We observed much better transmission level and stability to manufacturing tolerances for a loaded waveguide configuration than for an open structure. Thus, we are using a MTM-loaded waveguide configuration for our studies.

In Ref. 19, we discussed some theoretical aspects of par-

^{a)}Author to whom correspondence should be addressed. Electronic mail: antipov@anl.gov. Presently at Argonne National Laboratory.

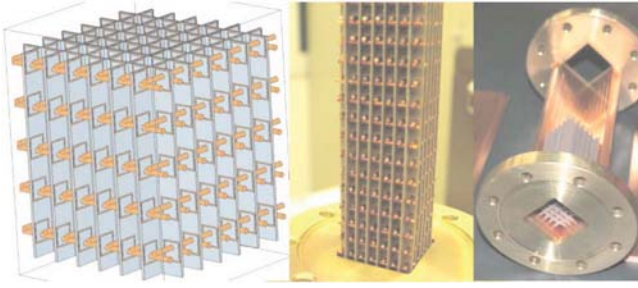


FIG. 1. (Color online) Left: MTM drawing. Center: picture of a manufactured MTM. Right: waveguide with alignment grooves.

interaction with a MTM placed in a waveguide. For the case of a loaded waveguide, CR generated by charged particle propagation through the structure is usually called a *wakefield*, in analogy to the wake generated behind a boat on a river. We developed a simulation approach to determine the frequency and the level of excitation of waveguide modes from a charged particle beam. Interesting properties of CR in a dispersive and anisotropic medium can be utilized for particle detection.^{2,3,19}

In this paper, we begin by reviewing the design and implementation of the TM₁₁-mode based MTM-loaded waveguide. Cold tests of the MTM-loaded waveguide demonstrated a left-handed band at 10 GHz frequency. We then report on our first beam test of the waveguide. In this experiment, a 6 MeV, $\frac{1}{4}$ nC electron beam passed through the MTM-loaded waveguide. We determined that a 10 GHz component was excited in the wakefield spectrum. This is an indirect demonstration of wakefield generation in a left-handed band. The frequency response of the beam data matched the left-handed frequency band demonstrated in the cold test, but explicit verification of the direction of propagation has not yet been done. Direct demonstration could be performed with a multiprobe measurement or the employment of a directional coupler. For this first experiment, loose manufacturing tolerances and probe calibration issues prevented us from making a decisive statement that the radiation was backward. However, the beam data are consistent with the cold test measurements.

II. DESIGN OF THE METAMATERIAL-LOADED WAVEGUIDE

For the MTM design, we picked a typical SRR and wire array configuration. We have SRRs and wires arranged in a two-dimensional (2D) grid (see Fig. 1). In this way, we have MTM elements aligned along both x and y directions. This is done to match TM₁₁ mode field patterns. We will assume a waveguide to be aligned longitudinally with the z axis. The effective tensors for permeability and permittivity are as follows:

$$\hat{\epsilon} = \begin{pmatrix} \epsilon_{\perp} & 0 & 0 \\ 0 & \epsilon_{\perp} & 0 \\ 0 & 0 & \epsilon_{\parallel} \end{pmatrix}, \quad \hat{\mu} = \begin{pmatrix} \mu_{\perp} & 0 & 0 \\ 0 & \mu_{\perp} & 0 \\ 0 & 0 & \mu_{\parallel} \end{pmatrix}, \quad (1)$$

$$\epsilon_{\perp} = 1 - \frac{\omega_{pe}^2}{2i\gamma_e\omega + \omega^2}, \quad \epsilon_{\parallel} = 1, \quad (2)$$

$$\mu_{\perp} = 1 + \frac{F\omega^2}{\omega_{rm}^2 - 2i\omega_{dm}\omega - \omega^2}, \quad \mu_{\parallel} = 1. \quad (3)$$

Dispersion parameters are controlled through the element geometry.^{6,7} It is important to note that design values are incredibly sensitive to the manufacturing tolerances. Also, there are several possible relative placements for the wire array and SRRs. We tried to manufacture the MTM to be symmetrical and uniform. However, some built-in asymmetries were unavoidable.¹⁸ Moreover, there are challenges with the usage of an effective medium approximation for the analysis. For example, a MTM exhibits a strong spatial dispersion at large wavelengths.²⁰ This makes predicted propagating bands below the cut off frequency of the waveguide^{19,21} practically unrealizable with a wire array.

The split rings were designed to have a resonance at around 9.5 GHz. They were produced by conventional PCB technology. Then, they were assembled into a beehive (cell) structure. Wires, made of 1 mm thick magnet wire, penetrate the split rings. The waveguide was chosen to be square (1.3×1.3 in.², cutoff frequency of ~ 6.2 GHz) rather than rectangular to maintain a TM₁₁ mode symmetry closer to that of a circular waveguide. It was manufactured having small grooves (see Fig. 1) to hold the MTM PCBs. For the TM₁₁ mode, such grooves are not destructive since the surface currents are longitudinal. Such grooves with small modifications can even act as dipole mode suppressors.²²

III. BENCH MEASUREMENTS OF THE TM₁₁ MODE PROPAGATION THROUGH METAMATERIAL-LOADED WAVEGUIDE

A. Mode launcher design

For cold tests, we used a standard HP8510C network analyzer. The source from the network analyzer is an electromagnetic pulse that is transformed to a particular mode or modes of the structure under test. This transformation is done by a mode launcher. We had to design and custom make the TM₁₁ mode launcher. The geometry of the antenna has to provide a symmetry that corresponds to the field distribution (see Fig. 2) of the mode of interest. We used MICROWAVE STUDIO (Ref. 23) to design the mode coupler. The geometry of the TM₁₁ launcher is simple. At the center of the waveguide aperture, there is a coax center pin with a tuning disk at the end. There is a conducting wall behind it, which is connected to the coax outer shell (ground).

As part of the mode launcher design process, we performed parametric simulations for different pin lengths, tuning disk thickness, and radii. The result of the simulation is the transmission (conversion) of the Transverse Electromagnetic (TEM) mode of the coaxial into the TM₁₁ mode of the waveguide. Some of the results are presented in Fig. 2. We were able to create a reasonably flat, low reflection region between 6.5 and 11.5 GHz. We confirmed through simulations that the remaining (not transmitted) power gets reflected rather than coupled into other modes. The parameters of the manufactured mode launcher are as follows: pin length of 0.15 in., radius of 0.07 in., and thickness of 0.02 in. Parametric analysis also shows that manufacturing tolerances

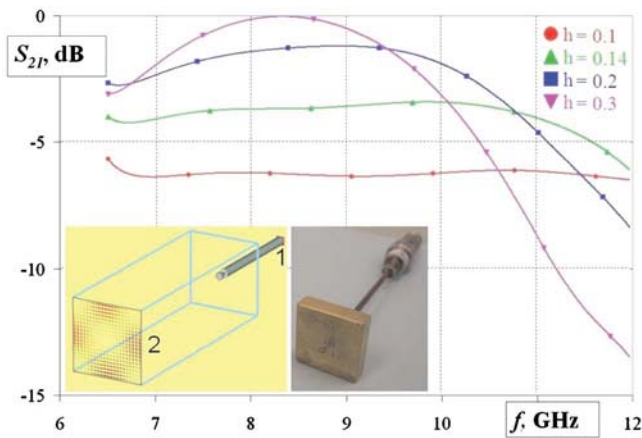


FIG. 2. (Color online) Parametric simulations of mode launcher varying the length of the pin h (inches). The plots show transmission from the coaxial cable into the TM_{11} mode of the waveguide for various pin lengths. The insets show the design drawing and a picture of the manufactured mode launcher.

will affect only the level of the transmission but not the uniformity of the response as a function of frequency. This is acceptable for the type of measurements done on the waveguide structure.

We produced two TM_{11} mode couplers (source and receiver). Then, we performed typical transmission/reflection measurements of the waveguide loaded with (a) only split rings, (b) only the wire array, and (c) both split rings and the wire array (combined structure).

B. Transmission through the SRR-loaded waveguide

Large assemblies of SRRs demonstrate collective behavior, which results in a frequency broadening of the reflection line of the assembly. In the experiment, this effect is enhanced due to manufacturing tolerances and misalignments. Measured transmission as a function of frequency is shown in Fig. 3. The SRR-only structure exhibited a wide resonance between 8.5 and 10.5 GHz.



FIG. 3. Bench measurement of transmission of TM_{11} mode through the waveguide loaded only with SRRs. There is no transmission between 8.5 and 10.5 GHz due to resonance in SRRs ($\mu < 0$).

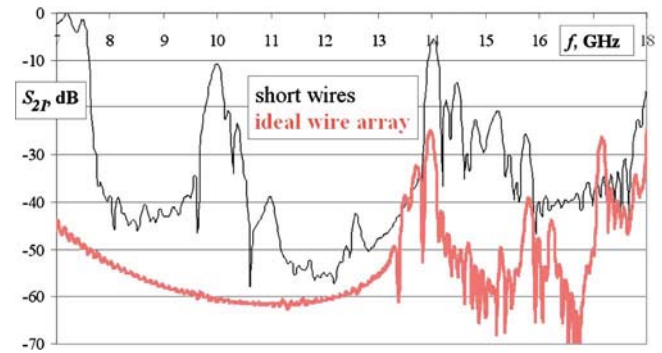


FIG. 4. (Color online) Transmission of TM_{11} mode through the waveguide loaded with the wire array (simulation). The thick curve corresponds to the case of an ideal wire array (wires are connected to the waveguide walls). The thin curve corresponds to short wires. There is a capacitive gap between the tip of each wire and a waveguide wall. Hence, the undesirable transparent region near 10 GHz.

C. Transmission through the wire array-loaded waveguide

A wire array proved to be a robust configuration for the TE_{10} mode in our previous experiments.¹⁷ For the TM design, the wire array was assembled in a 2D array. Due to the large number of the elements in the array and vacuum requirements, we were unable to drill holes through the waveguide walls and place the wires all the way through. This created a problem; we could not ensure proper contact between each single wire and the waveguide walls. A small capacitive gap between the tip of the wire and the waveguide wall combined with the wire's self-inductance formed a resonant circuit, similar to that of the CLS geometry discussed in Ref. 9. This made the system very sensitive. The wires could move, changing the effective capacitances between their tips and waveguide walls. Simulation results in Fig. 4 show the difference between an ideal wire array (having a design plasma frequency between 12 and 14 GHz) and short wires. A resonant transmission peak appears for the short wires in what would otherwise be a plasmlike suppression region.

There are 420 wires in the MTM. It is practically impossible to make them all the same length when assembling the structure by hand. In the first construction of the MTM, the length variation was not carefully controlled. So, there was a large spread in CLS-type resonant frequencies and a clear suppression region could not be defined (see Fig. 5). For the second construction of the wire array, a conscious effort to make the wires the same length was made. This created a strong resonant transmission peak around 9 GHz. On the positive side, the measurement became much more stable with better defined suppression regions (regions of negative ϵ) between 8 and 9 GHz and around 10 GHz (see Fig. 5).

D. Transmission through combined structure

With the improved wire array, we were able to identify the left-handed region for the combined structure. In this region, there is a resonant transmission drop for the SRR-only structure. The wire array exhibits a plasmlike behavior, suppressing transmission over a broader range of frequencies, except with a resonant transmission peak due to addi-

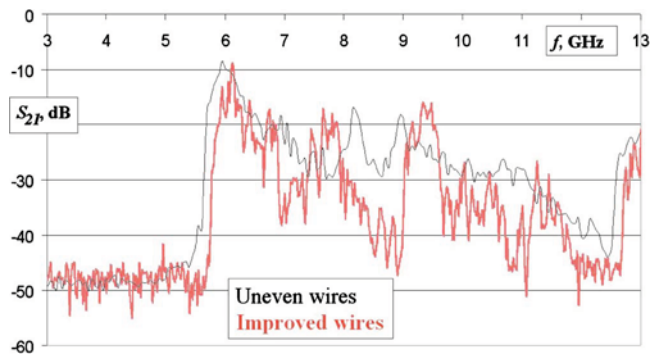


FIG. 5. (Color online) Transmission of the TM_{11} mode through the waveguide loaded with the wire array (bench measurement). The thin line corresponds to wires with large variation of length. The plasmlike behavior is washed out by the transparent regions. The thick line represents the case of wires that have almost the same length. In this case, there are better defined regions of suppressed transmission (8–9 GHz and 9.5–11 GHz). Note that there is no overcritical propagation.

tional capacitance between the waveguide wall and tips of the wires. The combined structure shows transmission in the region near 10 GHz (see Fig. 6), where neither the SRR structure ($\mu < 0$) nor the wire array ($\epsilon < 0$) have transmission. To our knowledge, this is the first left-handed MTM-based TM_{11} mode waveguide designed and experimentally tested.

IV. MEASUREMENT OF WAKEFIELD GENERATED BY AN ELECTRON BEAM PASSING THROUGH THE METAMATERIAL-LOADED WAVEGUIDE

The vacuum compatibility of the MTM substrates is not known. Therefore, the MTM waveguide was placed at the end of the beamline in a separate vacuum system. The MTM “beamline” contained a foil screen (for vacuum isolation) and a cross for vacuum pumping access. A phosphor screen was also placed in the cross to confirm that the beam made it through the waveguide (see Fig. 7). Integrated charge transformers exist at different locations along the beamline. They provide data on the total charge per bunch.

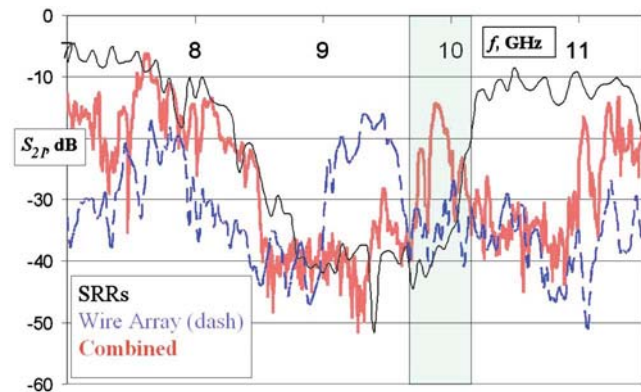


FIG. 6. (Color online) Combined bench measurement data. Transmission of the TM_{11} mode through the waveguide loaded with SRRs (thin solid line), through the wire array (thin dashed line) and through the combined structure (wire array+SRRs) (thick line). The combined structure has a transmission peak in the region of 9.7–10.2 GHz, where neither SRRs nor wires exhibited transmission. This is the signature of left-handed band.

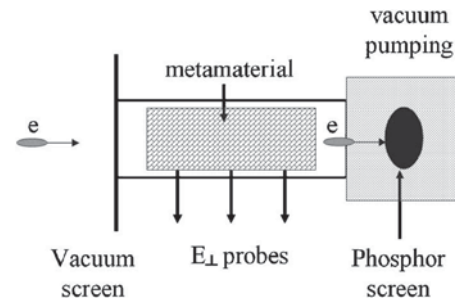


FIG. 7. Setup for beam test. Electron bunches pass through the waveguide loaded with MTM from left to right. The generated wakefield is picked up by voltage probes on the waveguide walls. To verify that the electron beam passed through the structure, the beam image is monitored on a phosphor screen located behind the waveguide. The whole system is under vacuum to avoid air ionization by electrons that would produce additional background noise.

We had a 0.25 nC, 3 mm (10 ps) longitudinal size beam passing through the MTM waveguide. The generated signal was picked up by side wall probes (see Fig. 7). It had to be attenuated before reading it with an oscilloscope. On the oscilloscope, we observed time resolved voltage signals (wakefield) from the waveguide side wall probes.

We performed a Fourier transform of the signal to obtain spectral data and then compare it to the data from the cold test. We can clearly see a wakefield excitation at around 10 GHz (see Fig. 8). As we demonstrated previously with the network analyzer (cold) test, the 10 GHz region is the double-negative region (see Fig. 6). Therefore, this measurement is the first indirect demonstration of reversed CR in a quasicontinuous medium (a MTM, as opposed to corrugated waveguides used in backward wave oscillators). To demonstrate the backward mode directly, we have to perform a measurement with multiple probes. This measurement requires precise calibration of probes. While we did perform multiple probe measurements, manufacturing tolerances, probe and cable calibration requirements, and beam fluctuations made it practically impossible to make a decisive statement as to whether we observe a backward mode directly or not.

V. APPROXIMATE THEORETICAL MODEL FOR THE EXPERIMENT

It is not possible to make a direct comparison of the experimental results to an accurate numerical model for two reasons. As stated earlier, due to limited computer resources, it is impossible to make a full scale simulation of the multimedia structure. In addition, resonant structures based on split rings are known to be very sensitive to manufacturing tolerances. Therefore, in the following, we present an approximate model of the experimental structure to provide a qualitative explanation of the measurement.

We tried to manufacture the MTM to be symmetrical and uniform. However, some asymmetries were unavoidable. One major problem was that the two sets of wires (in the x and y directions) could not physically intersect. Therefore, they penetrated the split rings in two different locations with respect to the ring element geometry. In this way, two sets of split rings were created: one with the wire penetrating the

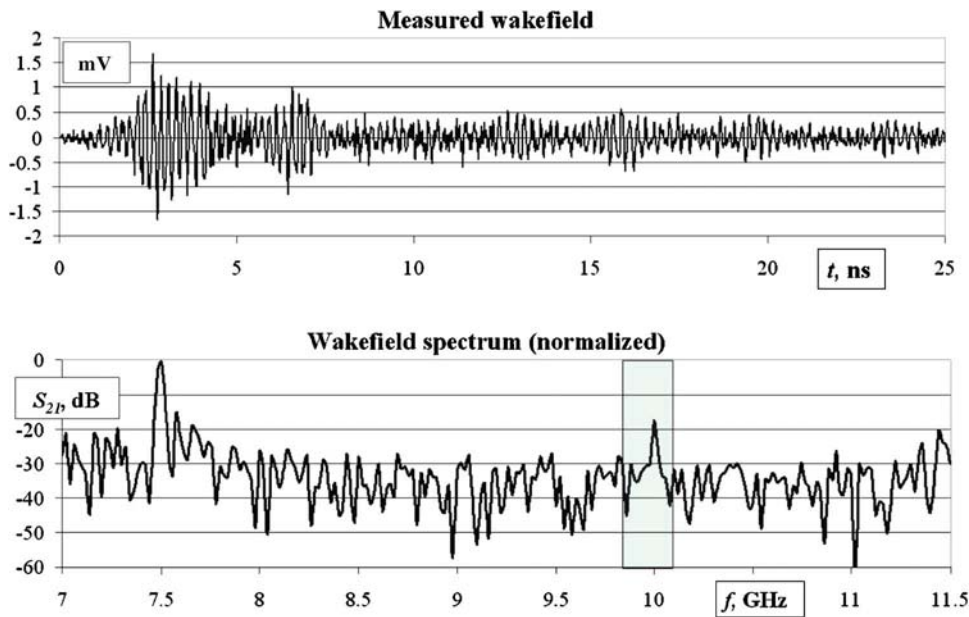


FIG. 8. (Color online) Results of the beam test: single voltage probe measurement. The top portion of the figure shows the time dependent amplitude of the wakefield measured upon passage of the electron bunch. The bottom shows the normalized frequency spectrum of the wakefield. We observe that the wakefield has a measurable 10 GHz peak above the noise floor. This corresponds to response of the structure in the left-handed band.

ring close to the capacitive cut and the other with the wire penetrating far away from the cut. These two sets of split rings have two different resonant frequencies. Hence, we chose the permeability of the model to have two additive quasi-Lorentz terms with different resonant frequencies. The negative region lies between 8.5 and 10 GHz (see Fig. 9) and corresponds to a drop in transmission during the bench test (see Fig. 3).

Ideally, in a long wavelength approximation, the wire array has as plasmlike behavior. However, due to the finite length of the wires, there is also a capacitive region between the wire tips and the waveguide wall. Due to this capacitive region and the self-inductance of the wire, a resonant transmission region was observed during the bench test (see Figs. 4 and 5). The permittivity was modeled as plasmlike with the addition of a Lorentz term, corresponding to the transmission band in the experimental test (see Figs. 5 and 9).

Based on this model, we calculated the dispersion relation for the TM_{11} mode in our waveguide (see Fig. 10). There are two possible points for mode excitation by an ultrarelativistic electron. The excitation at around 7.5 GHz has

a positive group velocity, while the one at around 10 GHz has a negative group velocity. The parameters of the theoretical model are *chosen* to fit the experimental data to provide a qualitative explanation of the measurement.

VI. SUMMARY

MTM-loaded waveguides have potential applications as higher order mode absorbers and beam position monitors. Theoretically, the reverse Cherenkov effect in left-handed MTMs has interesting properties for particle detection. The strength of artificially constructed double-negative MTMs is that they may be customized to exhibit a unique electromagnetic response not available in natural materials. In this paper, we presented experimental results of a charged particle beam interaction with double-negative MTM structure.

Our previous theoretical and simulation work¹⁹ on double-negative MTM-loaded waveguides has now been followed up with experimental measurements. We designed a 2D MTM for a TM-mode based waveguide. We performed cold tests with a network analyzer and demonstrated a left-handed band for the TM_{11} mode at around 10 GHz fre-

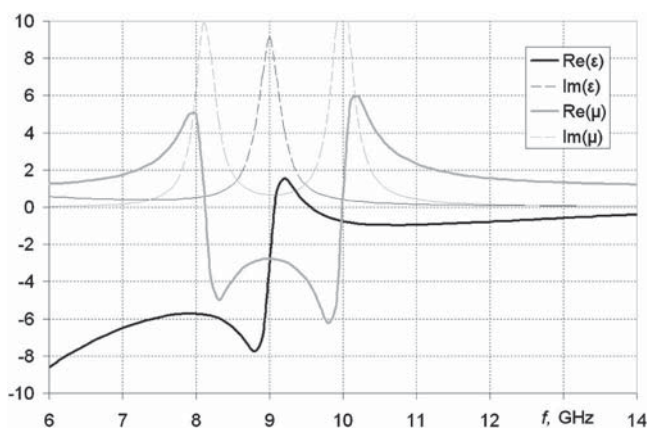


FIG. 9. Model of the medium parameters.

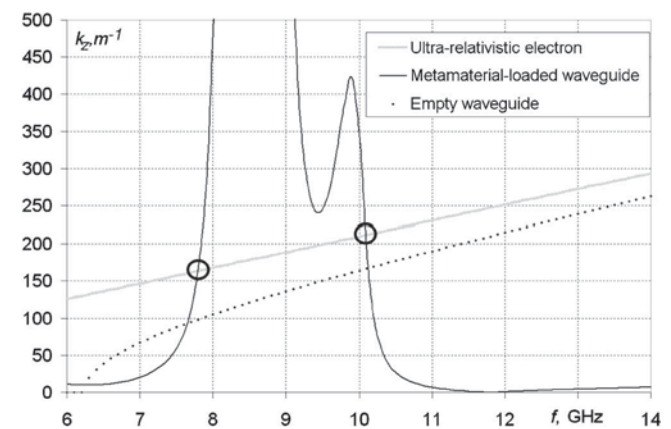


FIG. 10. Dispersion of the waveguide, loaded with dispersive medium (Fig. 9), dispersion of an empty waveguide and a particle dispersion.

quency. These were followed up with particle beam tests that showed generation of a strong signal in left-handed band at 10 GHz. This is an indirect demonstration of wakefield generation in left-handed band. To demonstrate the backward radiation directly, some modifications of the design are needed to address issues of manufacturing tolerances and filtering of frequency content imposed by probes and cables.

ACKNOWLEDGMENTS

This work was partially supported by the U.S. DOE, Division of High Energy Physics under Contract No. DE-AC02-06CH11357 and National Science Foundation under Grant No. 0237162.

- ¹V. G. Veselago, *Sov. Phys. Usp.* **10**, 509 (1968).
- ²J. Lu, T. M. Grzegorzczak, Y. Zhang, J. Pacheco, B. I. Wu, J. A. Kong, and M. Chen, *Opt. Express* **11**, 723 (2003).
- ³Yu. O. Averkov, and V. M. Yakovenko, *Phys. Rev. B* **72**, 205110 (2005).
- ⁴A. V. Tyukhtin, S. P. Antipov, A. Kanareykin, and P. Schoessow, *IEEE Proceedings of the PAC*, 2007 (unpublished), pp. 4156–4158.
- ⁵R. Shelby, D. R. Smith, and S. Schultz, *Science* **292**, 77 (2001).
- ⁶J. B. Pendry, A. J. Holden, D. J. Robbins, and W. J. Stewart, *IEEE Trans. Microwave Theory Tech.* **47**, 2075 (1999).
- ⁷J. B. Pendry, A. J. Holden, W. J. Stewart, and I. Youngs, *Phys. Rev. Lett.* **76**, 4773 (1996).
- ⁸W. Rotman, *IRE Trans. Antennas Propag.* **10**, 82 (1962).
- ⁹R. W. Ziolkowski, *IEEE Trans. Antennas Propag.* **51**, 7 (2003).
- ¹⁰D. R. Smith, W. J. Padilla, D. C. Vier, S. C. Nemat-Nasser, and S. Schultz, *Phys. Rev. Lett.* **84**, 4184 (2000).
- ¹¹A. Grbic and G. V. Eleftheriades, *J. Appl. Phys.* **92**, 5930 (2002).
- ¹²I. Arnedo, J. Illescas, M. Flores, T. Lopetegui, M. A. G. Laso, F. Falcone, J. Bonache, J. García-García, F. Martín, J. A. Marcotegui, R. Marqués, and M. Sorolla, special issue of *IET Proc. Microwaves, Antennas Propag.* **1**, 65 (2007).
- ¹³Argonne Wakefield Accelerator Facility website (www.hep.anl.gov/awa).
- ¹⁴T. J. Yen, W. J. Padilla, N. Fang, D. C. Vier, D. R. Smith, J. B. Pendry, D. N. Basov, and X. Zhang, *Science* **303**, 1494 (2004).
- ¹⁵C. M. Soukoulis, *Science* **315**, 47 (2007).
- ¹⁶S. Antipov, W. Liu, J. Power, and L. Spentzouris, *IEEE Proceedings of the PAC*, 2005 (unpublished), pp. 458–460.
- ¹⁷S. Antipov, W. Liu, W. Gai, J. Power, and L. Spentzouris, *AIP Conf. Proc.* **877**, 815 (2006).
- ¹⁸S. Antipov, W. Liu, W. Gai, J. Power, and L. Spentzouris, *Nucl. Instrum. Methods Phys. Res. A* **579**, 915 (2007).
- ¹⁹S. Antipov, W. Liu, W. Gai, J. Power, and L. Spentzouris, *J. Appl. Phys.* **102**, 034906 (2007).
- ²⁰P. A. Belov, R. Marques, S. I. Maslovski, I. S. Nefedov, M. Silveirinha, C. R. Simovski, and S. A. Tretyakov, *Phys. Rev. B* **67**, 113103 (2003).
- ²¹V. A. Podolskiy and Ev. E. Narimanov, *Phys. Rev. B* **71**, 201101(R) (2005).
- ²²E. Chojnacki, W. Gai, C. Ho, R. Konecny, S. Mtingwa, J. Norem, M. Rosing, P. Schoessow, and J. Simpson, *J. Appl. Phys.* **69**, 6257 (1991).
- ²³CST, *Microwave Studio Manual* (<http://www.cst.com/>).